Pectoral and pelvic girdle rotations during walking and swimming in a semi-aquatic turtle: testing functional role and constraint

Christopher J Mayerl*[1]

John G Capano[2]

Adam A Moreno[2]

Jeanette Wyneken[3]

Richard W Blob[4]

Elizabeth L Brainerd[2]

[1]Department of Anatomy and Neurobiology, Northeast Ohio Medical University (NEOMED), Rootstown, OH, 44272, USA

[2]Department of Ecology and Evolutionary Biology, Brown University, Providence, RI, 02912, USA

[3]Department of Biology, Florida Atlantic University, Boca Raton, FL, 33431, USA

[4]Department of Biological Sciences, Clemson University, Clemson, SC, 29634, USA

* Author for correspondence: cmayerl@neomed.edu

Keywords: biomechanics, morphology, locomotion, X-ray reconstruction of moving morphology

Summary statement: During locomotion, the turtle pectoral girdle rotates more than the pelvis. While pelvic girdle rotations are larger on land, the pectoral girdle rotates similarly during swimming and walking.

Abstract

Pectoral and pelvic girdle rotations play a substantial role in enhancing stride length across diverse tetrapod lineages. However, the pectoral and pelvic girdle attach the limbs to the body in different ways and may exhibit dissimilar functions, especially during locomotion in disparate environments. Here, we test for functional differences between the forelimb and hind limb of the freshwater turtle *Pseudemys concinna* during walking and swimming using X-Ray Reconstruction of Moving Morphology (XROMM). In doing so, we also test the commonly held notion that the shell constrains girdle motion in turtles. We found that the pectoral girdle exhibited greater rotations than the pelvic girdle on land and in water. Additionally, pelvic girdle rotations were greater on land than in water, whereas pectoral girdle rotations were similar in both environments. These results indicate that although the magnitude of pelvic girdle rotations depends primarily on whether the weight of the body must be supported against gravity, the magnitude of pectoral girdle rotations likely depends primarily on muscular activity associated with locomotion. Furthermore, the pectoral girdle of turtles rotated more than has been observed in other taxa with sprawling postures, showing an excursion similar to that of mammals (~38°). These results suggest that a rigid axial skeleton and internally positioned pectoral girdle have not constrained turtle girdle function, but rather the lack of lateral undulations in turtles and mammals may contribute to a functional convergence whereby the girdle acts as an additional limb segment to increase stride length.

Introduction

The evolution of robust limb girdles is thought to have played a key role in the ability of tetrapods to move on land (Coates et al., 2002). The most well-known role of these girdles is to support the weight of the body during locomotion (Carrier, 2006). However, tetrapod girdles also can work in conjunction with movements of the body axis and the limbs to increase stride length during locomotion (Boczek-Funcke, 1996; Jenkins and Goslow Jr., 1983; Jenkins and Weijs, 1979; Nyakatura and Fischer, 2010; Peters and Goslow Jr., 1983; Veeger and van der Helm, 2007). As a result, the girdles undergo tradeoffs between being supportive and stable, but also mobile. Although these roles are widely recognized, two variables may impact the relative significance of the role of the girdles in body support compared to increasing stride length. First, there are differences between the forelimbs and hind limbs in how each girdle attaches the limbs to the body; second, tetrapods have radiated to occupy a variety of environments, and the physical properties of those environments may influence the importance of body support.

The pectoral and pelvic girdle attach the limbs to the body in two different and distinct ways. The pelvic girdle articulates with the sacral vertebrae directly via the sacro-iliac joint. In contrast, the tetrapod pectoral girdle articulates with the body primarily via a muscular sling, whereby the girdle is generally attached via a series of muscles and ligaments to the rib cage, which is then attached to the vertebrae. Additionally, in many species there is a ventral connection between the sternum and clavicle. Despite these fundamental differences, both girdles must support the body during terrestrial locomotion (Carrier, 2006; Mayerl et al., 2016). Furthermore, both girdles rotate during locomotion to enhance stride length (Baier et al., 2018; Jenkins and Goslow Jr., 1983; Mayerl et al., 2016; Pridmore, 1992). However, distinguishing the role of body support from the role of enhancing stride length is challenging in most tetrapods. The relative influences of these functions can be decoupled by studying girdle function in water, where the animal does not have to support the body against gravity. However, most semiaquatic tetrapods use different parts of their body to move in

aquatic and terrestrial environments. For example, semiaquatic lizards and crocodiles swing their limbs and use axial undulations during terrestrial locomotion, yet primarily generate propulsion via axial and tail undulations during aquatic locomotion, although some vertebrates, including turtles utilize bottom-walking as well (Ashley-Ross and Bechtel, 2004; Fish, 1984; Lindgren et al., 2010; Ringma and Salisbury, 2014; Zug, 1972).

One lineage of vertebrates that is particularly tractable for comparisons of girdle function across locomotor environments is turtles. The ankylosing of the vertebrae within the dorsal part of the shell (carapace) results in all thrust for locomotion being generated by limb movements and, potentially, by the girdles to which the limbs attach (Mayerl et al., 2016; Pace et al., 2001). Freshwater representatives of this lineage also use similar craniocaudal limb motions on land and in water, facilitating comparisons of limb and girdle function. Furthermore, despite the presence of the bony shell, the girdles of turtles attach to the body in a similar manner to that of other tetrapods. The pelvic girdle of most turtles attaches to the vertebral column by paired, fibrous sacro-iliac joints, whereas the pectoral girdle attaches to the trunk via ligamentous connections ventrally (acromion processes to the plastron) and dorsally (suprascapular cartilages to the pleural bones and anterior trunk vertebrae), as well as via muscles that originate on the scapulae, acromion processes and procoracoids (Walker, 1973). Some of the intrinsic and extrinsic musculature of the pectoral girdle has migrated in turtles (Nagashima et al., 2009), but the functional connections of the girdles to the body are similar to those of other tetrapods. Despite this, a synapomorphy of turtles is that their girdles lie internal to the ribcage (Burke, 1989), which is fully contained inside the shell (Fig. 1). This structural distinction of turtles has been viewed as a feature that places functional constraints on their locomotor system (Walker, 1971).

Here, we use X-ray Reconstruction of Moving Morphology (XROMM) to answer three questions about the locomotor function of the limb girdles using a generalist species of freshwater turtle, the river cooter (*Pseudemys concinna*, LeConte 1830). (1) Does the pectoral girdle, with its

ligamentous attachment to the body, rotate more than the pelvic girdle? (2) Is there an impact of environment on girdle and limb function during locomotion in turtles? And, (3) does the location of the girdles inside of the shell constrain locomotor function in turtles? By focusing on a lineage that uses the same structures to locomote through multiple environments, we seek to gain general insight into tetrapod girdle and limb function, as well as test how the media through which an animal moves can impact the function of its locomotor system.

Materials and methods

The analyses detailed in this study synthesize newly collected XROMM results from measurements of pectoral girdle and limb function with new analyses of previously collected XROMM data on pelvic girdle and limb function (Mayerl et al., 2016). Detailed information on methods associated with the pelvic dataset can be obtained from the previously published study (Mayerl et al., 2016); here, we detail methods specifically relating to pectoral function and new data extracted from the previously collected pelvic recordings.

Experimental animals

Three adult male *P. concinna* (mass: 613g, 682g, 1028g, straight carapace length: 17.5cm, 18.7cm, 20.6cm, respectively) were collected from a spillway of Lake Hartwell, Pickens County, SC USA using hoop nets (South Carolina Scientific Collection permit # 28 -2016). Turtles were housed in 600 L stock tanks equipped with dry basking platforms and pond filters in a temperature-controlled greenhouse facility; they were fed commercial reptile pellets daily. For XROMM data collection, turtles were transported to Brown University (Providence, RI USA). All animal care and experimental procedures were approved by the Institutional Animal Care and Use Committees (IACUC) of Clemson University (protocol 2015-001) and Brown University (protocol 1105990018).

Surgical procedures

Surgical procedures for the forelimb followed those performed on the hindlimb (Mayerl et al., 2016).Two weeks prior to data collection, turtles underwent a surgical procedure at Clemson University to implant 1 mm radio-opaque tantalum bead markers (Bal-Tec, Los Angeles, CA) into the humerus, pectoral girdle, and shell (3-5 markers per bone) using aseptic technique. Doses of 1 mg kg^{-1} butorphanol, 90 mg kg^{-1} ketamine and 1 mg kg^{-1} xylazine were injected into the muscles of the right forelimb to induce analgesia and a surgical plane of anesthesia. A single incision was made along the cranial aspect of the left forelimb and adjacent body wall to allow access to the pectoral girdle and humerus. Muscles were separated along fascial planes to expose the surfaces of the bones (Mayerl et al., 2016), and a small 'window' of periosteum was removed using a periosteal elevator to expose bone cortex at locations of marker implantation. Each marker was implanted by hand-drilling a 1 mm diameter hole into the bone and subsequently inserting the bead into the hole with the end of a wooden applicator stick. We maximized the distance between the markers in each bone to help optimize the accuracy and precision of reconstructions of movement (Brainerd et al., 2010). Girdle markers were placed in the acromion (one bead medially, and one bead laterally ventral to the glenohumeral joint) and scapula (one bead dorsally, one bead ventrally, dorsal to the glenohumeral joint, Fig. 1). Humeral markers were placed in proximal and midshaft regions as well as the distal condyles (Fig. 1). Following marker implantation, incisions were sutured closed, and turtles were allowed to recover on land for 24 hours before being placed in an individual aquatic enclosure with a basking platform.

Data collection

Data were collected following standard marker-based XROMM protocols (Brainerd et al., 2010). At the beginning, middle, and end of each day of data collection, standard undistortion grids and 3-dimensional calibration cube images were collected (Brainerd et al., 2010). Turtles were recorded

during steady walking (6.0 – 10.6 $cm*s^{-1}$) and swimming (7.2 – 11.8 $cm*s^{-1}$) using biplanar X-ray video with two X-ray generators (Imaging systems and Service, Painesville, OH USA) set at 90-105 kV and 100 mA. Videos were recorded at 100 fps for walking and 150 fps for swimming using Phantom v. 10 high-speed cameras (Vision Research, Wayne, NJ USA) at a 1760x1760 pixel resolution with a 1/1000s shutter speed. During walking, the X-ray generators and cameras were positioned in dorsal and lateral views, and animals were filmed as they walked on a hand-powered treadmill, which minimized magnetic interference. This allowed turtles to walk at self-selected speeds which were similar for forelimb and hindlimb trials. During swimming, X-ray generators and cameras were placed in oblique views angled at 45° to the plane of animal movement and orthogonal to each other. Turtles were video recorded as they swam through 10 cm deep water (approximately twice the depth of the shell), from one end of a 161 x 61 cm acrylic aquarium to the other. This depth was deep enough to ensure the turtles were not touching the bottom of the tank or exposed to the air, while enabling maximal penetration for X-Ray images. In both environments, turtles were allowed to rest for approximately 10 min between trials and a minimum of five limb cycles were collected per individual per environment (N > 15 cycles per environment).

Following the last day of biplanar X-ray video data collection, turtles were sedated using an intramuscular injection of ketamine (30 mg kg^{-1}) and computed tomography (CT) scans were taken of each individual with an Animage Fidex veterinary scanner with an 8-15 cm field-of-view and 0.2 – 0.3 mm isotropic voxels (Fidex, Animage, Pleasanton, CA USA). CT scans were subsequently used to generate polygonal mesh models of the shell, pectoral girdle, and humerus of each turtle in OsiriX (Fig. 2, v. 3.9.2 64 bit, Pixmeo, Geneva, Switzerland), which were cleaned using Geomagic Design X64 (v. 2016 0.1, Geomagic, Triangle Park, NC USA).

Data processing and precision

X-ray videos and the associated undistortion and 3-D calibration images were processed using open source software XMALab v.1.5.1 (https://bitbucket.org/xromm/xmalab/; (Knörlein et al., 2016). Following undistortion and calibration, markers were identified from X-ray images and tracked. Markers located on the same bone (3-5 markers per bone) were grouped into rigid bodies, and the filtered motions of these rigid bodies were exported using a first-order low-pass Butterworth filter (12Hz cut off). Marker tracking precision can be quantified by the standard deviation of the intermarker distance within a rigid body (Brainerd et al., 2010; Cieri et al., 2018). For the hindlimb during walking and swimming and the forelimb during walking, mean marker tracking precision was 0.1 mm with a range of 0.05 mm to 0.3 mm. Mean marker tracking precision for the forelimb during swimming was 0.06 mm, with a range of 0.04mm to 0.09 mm. Animations were constructed by applying rigid body motions to polygonal mesh models of the bones in Autodesk Maya 2017 (San Rafael, CA USA) using the XROMM MayaTools (https://bitbucket.org/xromm/xromm_mayatools/).

To describe the motion of the shell, pectoral girdle, and humerus, we created Anatomical Coordinate Systems (ACSs) for each bone by setting a reference pose to be used as a zero point that was standardized across individuals. For the pectoral girdle ACS, we used the orientation of the scapular and acromial processes to set the reference posture (Fig. S1 A,B). We positioned the scapular process to extend dorsally, perpendicular to the plastron at the midline of the animal. The acromion process was rotated to point cranially, parallel with the midline and plastron. We centered the pectoral ACS at the dorsal tip of the scapular process, and aligned it so that the x-axis was parallel with the plastron and oriented perpendicular to the long-axis of the turtle, the z-axis was oriented to a line connecting the distal ends of the scapula and acromion, which resulted in a y-axis that pointed cranially and dorsally. To measure movements of the pectoral girdle, we created a second ACS in the same orientation and measured movements relative to the shell, rather than the

girdle. We then created a joint coordinate system (JCS) between these two ACSs to track the movements and rotations of the pectoral girdle relative to the shell using the XROMM MayaTool 'oRel' (Brainerd et al., 2010; Menegaz et al., 2015)). This resulted in movements of the pectoral girdle relative to the shell to be measured as pitch (x-axis), roll (y-axis) and yaw (z-axis).

To measure humeral movements, the reference pose was oriented so that the long axis of the humerus was perpendicular to the scapula and acromion with the concave surface facing ventrally (Fig. S1 C,D). We centered the ACS on the glenohumeral joint by measuring it relative to a small sphere that fit the head of the humerus. The ACS was oriented so that the x-axis was aligned through the long axis of the humerus, the y-axis was oriented to point cranio-caudally parallel to the midline of the plastron, and the z-axis was oriented to point dorso-ventrally, parallel to the scapula. To measure motions of the humerus relative to the girdle, we made a JCS by creating a second ACS in the same orientation and parented one ACS to the humerus, and the other to the pectoral girdle. This resulted in movements of the humerus being measured as long-axis rotation (x-axis rotation), abduction/adduction (y-axis rotation) and protraction/retraction (z-axis rotation). All angles were measured as Euler angles with a zyx rotation order for all bones.

To measure girdle contributions to protraction/retraction in both the humerus and the femur, we created locators on the distal end of the humerus and femur, as well as locators at the center of the glenohumeral joint and the acetabulum. We output the movements of these locators relative to the shell, and then divided the total amount of craniocaudal movement (protraction/retraction) of the limb bone locator by the craniocaudal movement of the girdle joint locator. All raw video data, CT scan data, and processed Maya scenes analyzed in this study were stored in accordance with best practices for video data management in organismal biology (Brainerd et al., 2017), and are available from the X-ray Motion Analysis Portal (xmaportal.org).

Statistical analyses

All statistical analyses were performed in R (V 3.2.1, www.r-project.org). We used linear mixed effects models to test for differences between limbs, during locomotor behavior (lme4; (Bates et al., 2015)). We used limb element (girdle or limb), behavior (swim or walk) and their interaction as fixed effects, with individual as a random effect. P-values were obtained using likelihood ratio tests of the full model with the effect in question against the model without the effect in question. We calculated effect sizes following published methods for mixed-effects models (Xu, 2003). Where interactions were significant, post-hoc analyses were conducted using a Tukey's correction to compare groups independently (R package 'emmeans'). All data are presented as mean ± standard error unless otherwise noted.

Results

Girdle rotations

We found substantial differences in the rotations exhibited by the pectoral and pelvic girdles, and in the extent of girdle rotation between aquatic and terrestrial environments for all individuals (Fig. 3, Fig. S2). In water and on land, yaw was the primary axis of rotation for both girdles, although both girdles rotated about all three axes of rotation (Fig. 4). Movements of the two girdles also exhibited different responses to changes in environment (Table 1). Rotations were more variable in the pectoral girdle than in the pelvic girdle during both swimming and walking (all Levene's tests $F > 10$, $p < 0.001$, Table S1). Pelvic girdle rotations during walking were approximately double those found during swimming for Rx (pitch), Ry (roll) and Rz (yaw) (Table 1, Table S1). In contrast, pectoral girdle rotations only differed between environments for pitch, in which walking steps had slightly (< 2.5°) greater rotations (Fig. 3, Table S1). Moreover, the pectoral girdle pitched substantially during both types of locomotion (swim: 12.6 ± 0.7°, walk: 14.8 ± 0.7°), whereas pelvic girdle pitch was less than

5° on average during swimming and walking (Table 1). The pectoral girdle also showed substantially greater yaw than the pelvic girdle, rotating by > 35° in both environments in comparison to 8.6 ±2.0° for the pelvic girdle in water and 18.2°±1.9° on land (Fig. 3, Table 1). Roll was minimal for both girdles (less than 5°) during both walking and swimming (Fig. 3, Table S1). JCS translations in all three dimensions were less than 0.2mm, below noise thresholds for precision in our previous work (Mayerl et al., 2016).

Limb rotations

The humerus and femur both underwent substantial rotations about all three axes in both environments for all individuals (Fig. S3, Table S2). Unlike in the girdles, forelimb (i.e., humeral) rotations differed between walking and swimming, and the forelimb did not exhibit consistently greater variation in rotational excursions than the hindlimb (Fig. 5). The two limbs were used differently during walking and swimming in abduction/adduction and in protraction/retraction (Table S3). The femur went through greater arcs of excursion for both Ry (abduction/adduction) and Rz (protraction/retraction) during walking than swimming, whereas rotations in Ry and Rz decreased in the forelimb during walking. In contrast, we found no interaction between limb and environment for long axis rotation of the limb (Rx), and both limbs underwent more long axis rotation (LAR) during walking than swimming (Fig. 5A).

LAR of the humerus was greater than the femur in both environments, and we found a significant effect of both limb and behavior ($p < 0.001$, swim humerus: 29.9 ± 2.7°, swim femur: 18.4 ± 2.4°; walk humerus: 44.7 ± 2.7°; walk femur: 34.3 ± 2.4°). Similarly, although humeral abduction/adduction and protraction/retraction excursion decreased in walking compared to swimming, both axes of rotation were larger in the humerus than the femur during swimming and walking (Fig. 5B, C). The primary axis of rotation for both limbs was protraction/retraction (Table S2). During swimming, the humerus went through an average of 123.6 ± 2.9° of rotation, which

decreased to 108.3 ±5.9° during walking. In contrast, mean femoral excursions increased from 70.4 ±5.5° during swimming to 89.6 ± 5.3° during walking.

Girdle contributions to limb protraction/retraction

In both the fore- and hind limb, the rotations of the girdles contributed to the total craniocaudal movement of the humerus (for the forelimb) and femur (for the hind limb), and girdle contributions were greater on land than in water for both limbs (Fig. 6, Table 2). Pectoral girdle rotations resulted in substantial craniocaudal movements at the glenoid, which led to glenoid movements contributing an average of 31.2 ± 1.7% of total craniocaudal movement at the distal humerus during swimming, and an average of 37.5 ± 1.7% during walking (Fig. 6, Movie 1, Table 2). In contrast, due to the smaller rotations of the pelvic girdle, rotations at the femoro-acetabular joint only contributed 8.2 ± 1.4% of the craniocaudal motions of the femur during swimming and 11.6 ± 1.3% during walking (Fig. 6, Table 2).

Discussion

Differences in rotation between the forelimb and hind limb

In *P. concinna*, pectoral girdle rotations were much greater than those of the pelvic girdle, especially lateral motions (yaw) associated with increasing stride length. These increased rotations result in the turtle shoulder girdle contributing to approximately 35% of the total arc of humeral craniocaudal motion, in contrast to the pelvic girdle, which only contributed 11.6% of femoral craniocaudal motions on average, similar to running frogs (Fig. 4, (Collings et al., 2019)). Schmidt et al., (2016) found that pectoral girdle rotations contributed approximately 35% of the arc of the humerus in the terrestrial tortoise, *Testudo hermanii*. These similarities indicate that the pectoral girdle of turtles plays a substantial role in enhancing stride length across turtles with different ecologies and phylogenetic histories (Schmidt et al., 2016).

Despite the similarities in the contribution of girdle rotation to humeral movements, pectoral girdle rotation magnitudes in *P. concinna* during swimming and walking, in the present study, were approximately double those measured in fully terrestrial tortoises (Schmidt et al., 2016). The smaller pectoral girdle rotations (~15°) found in tortoises could reflect an increased role of this girdle in body support related to their terrestrial habits, or potentially serve to stabilize the girdle during digging behaviors. The only previous evaluations of pectoral girdle yaw excursions in an aquatic turtle were from the painted turtle *Chrysemys picta*, a close relative of *P. concinna* from the clade Emydidae (Walker, 1971). Measurements in that study were obtained via two-dimensional cinefluroscopy during walking and showed pectoral yaw excursions of *C. picta* that were similar to those of tortoises (~16°). The same study found little evidence of pelvic girdle rotations suggesting that the increased rotations of the pectoral girdle could function to give the forelimb an overall excursion comparable to that of the hind limb, which is generally longer in freshwater turtles. However, because three-dimensional XROMM methods show that pelvic rotation does occur in *P. concinna* (Mayerl et al., 2016), it seems likely that differences between our pectoral girdle results for *P. concinna* and previous results for tortoises and painted turtles could be attributed to differences in the methods used to measure excursion (Schmidt et al., 2016; Walker, 1971). Previous measurements of pectoral girdle rotations quantified the two-dimensional angle of the scapular prong relative to the horizontal and mid-sagittal plane. Three-dimensional XROMM approaches can prevent underestimations of motion from two-dimensional methods, generating new insights into the relative motion of both girdles and how they compare across habitats and species.

The greater rotation of the pectoral girdle compared to the pelvic girdle may be attributed to differences in how each girdle attaches the limbs to the body. In most, but not all tetrapods, the pectoral girdle of tetrapods is connected to the trunk by muscles, tendons, and ligaments, as well as through a sterno-clavicular joint, whereas the pelvis is connected directly to the axial body via the sacro-iliac joint. Moreover, the left and right pelvic girdles tightly connect to each other in turtles, any connection between the left and right sides of the pectoral girdle is via very loose sheets of

connective tissue; the lack of a tight attachment may increase the potential for each pectoral girdle to act like an additional limb segment and increase stride length through its rotation, as in a variety of other tetrapods (Baier et al., 2018; Eaton, 1944; Fischer and Blickhan, 2006).

The impact of the environment on girdle movements

The two girdles showed a different functional response to locomotion in water and on land. Pectoral girdle rotations were large and of similar magnitude during both swimming and walking. In contrast, pelvic girdle yaw was twice as large during walking as during swimming. Given that pelvic girdle rotations change significantly depending on whether the body is supported by buoyancy, the greater yaw rotations of the pelvic girdle during terrestrial locomotion could reflect the need to support the body against gravity (Mayerl et al., 2016). In contrast, the lack of a difference in pectoral girdle rotation between water and land suggests that changes in the demands of body support have little influence on pectoral girdle movement in turtles, and that similarity of motion between habitats may be sustained by adjustments in patterns of muscle activity (Deban and Schilling, 2009; Delvolvé et al., 1997; Gillis and Blob, 2001; Mayerl et al., 2017; Rivera and Blob, 2010). In the freshwater turtle hindlimb and forelimb, retractor muscles generally exhibit greater amplitude bursts in activity during swimming than walking, which has been hypothesized to result from moving through a viscous medium (Blob et al., 2008; Gillis and Blob, 2001; Rivera and Blob, 2010). If muscle use drives girdle rotations, one would expect similar or greater rotations in water than on land, as we observed in the forelimb. In contrast, the decreased rotation of the pelvic girdle in water compared to land suggests that higher-amplitude contractile bursts during swimming do not result in increased girdle rotations, and that instead they function either to actively decrease rotations of the girdle, or that the role of supporting the body against the effects of gravity plays a larger role in driving pelvic girdle motions.

Comparisons of changes in limb motion between habitats

Long axis rotation (LAR) of the humerus and the femur were approximately 15° greater during walking than during swimming, suggesting that LAR plays a fundamentally similar role between the two limbs in both environments. Although the functional role of limb bone LAR is not fully understood, it is thought to enhance stride length and working space in a variety of both parasagittal and sprawling taxa (Ashley-Ross, 1994; Kambic et al., 2014; Kambic et al., 2015; Reilly and Delancey, 1997; Rewcastle, 1983). During swimming, freshwater turtles exhibit substantial long axis rotation of the distal elements of their forelimbs and hind limbs in order to effectively generate thrust during locomotion (Mayerl et al., 2017; Rivera and Blob, 2010), whereas during walking the distal elements of the limbs must be oriented roughly perpendicular to the substrate in order to support the animal on land (Mayerl et al., 2017). Thus, the smaller LAR of the proximal limb bones during swimming may reflect the greater rotation of other parts of the limb when moving in water, versus when pushing against solid substrates. The similar reduction of LAR between the humerus and the femur is surprising, given previous results on bone loading experiments in turtles that hypothesized that LAR would decrease more in the femur than in the humerus (Young and Blob, 2015; Young et al., 2017). In contrast, we found that LAR in both bones was reduced by a similar magnitude during swimming relative to walking, which suggests that the maintenance of twisting loads on the turtle humerus during swimming must result from some mechanism other than body suppport, such as how the limb interacts with the girdle or environment. It also is possible that load orientation in the limb bones changes non-linearly, and the higher absolute LAR in the humerus is still sufficient to maintain torsion in this bone during swimming (Young et al., 2017).

During protraction and retraction, the limbs differed in their excursion during walking compared to swimming. Humeral protraction/retraction decreased on land compared to in water, whereas femoral protraction/retraction excursion increased on land versus in water. These different patterns of use most likely reflect differences in how thrust is generated in each environment. In

water, thrust is generated by the limbs interacting with a fluid, and balancing the forces produced by contralateral sets of limbs is important for maintaining stable swimming (Jastrebsky et al., 2016; Mayerl et al., 2019; Rivera et al., 2006; Sefati et al., 2013). As the hindlimb of *P. concinna* has substantially greater surface area than the forelimb, the increased excursion of the forelimb during swimming might relate to increasing forces produced by that limb in order to balance the force produced by the hind limb (Mayerl et al., 2019; Walker, 1971). In contrast, on land thrust is produced by the limbs eliciting a reaction force from a solid substrate (Biewener and Patek, 2018). Thus, in terrestrial locomotion the limbs function to both support the body and to propel it, but the forces exerted by each limb do not directly result in destabilizing torques and are primarily vertical in turtles and other sprawling lineages (Blob and Biewener, 2001; Butcher and Blob, 2008; Zani et al., 2005). This reduces the need for balanced thrust generation between sets of limbs. Many terrestrial tetrapods are viewed as generating thrust primarily from one set of limbs (Alexander, 1974; Basu et al., 2019; Griffin et al., 2004; Raichlen et al., 2009; Shine et al., 2015), with sprawling amniotes such as turtles typically generating most thrust for terrestrial locomotion from the hind limb (Chen et al., 2006; McElroy et al., 2014; Willey et al., 2004). These findings are consistent with the differentiation in locomotor roles of the limbs suggested by our kinematic data, although research on species utilizing underwater walking would further delineate potential differences in limb function from differences in kinematic pattern.

The shell does not constrain girdle motion in turtles

Our results suggest that, contrary to previous assumptions, the presence of the shell does not constrain girdle function in turtles (Baier et al., 2018; Schmidt et al., 2016). Pectoral girdle rotations during terrestrial locomotion in *P. concinna* averaged 39° per stride. These rotations are much higher than in other sprawling taxa that have been studied (Baier and Gatesy, 2013; Baier et al., 2018; Fischer et al., 2010; Jenkins and Goslow Jr., 1983), causing rotations of the girdle to contribute more

to stride length in turtles than in other sprawling taxa, including those thought to have highly mobile pectoral girdles such as chameleons (8%) and alligators (11%) (Baier et al., 2018; Fischer et al., 2010). The enhanced pectoral mobility of these lineages has been attributed to the loss of the clavicle, which also is not present in turtles. In addition, chameleons and alligators exhibit decreased lateral undulations of the trunk during locomotion relative to other sprawling taxa, and a mobile sternocoracoid joint coupled with the loss of the clavicle, traits that have been proposed to enhance stride length and compensate for the lack of trunk rotations (Baier et al., 2018; Fischer et al., 2010). Due to the fusion of the vertebrae with the bony shell, turtles exhibit no lateral undulations of their vertebral column during locomotion, suggesting a significant role for the enhanced girdle rotations exhibited by *P. concinna*. Indeed, if pectoral girdle rotations (26°) and vertebral yaw (18°) in alligators are summed, they rotate by 44°, similar to the girdle yaw exhibited by turtles (Baier et al., 2018).

Despite a sprawling limb orientation, in some regards the turtle pectoral girdle may function more similarly to a mammalian shoulder than to that of other sprawling lineages. The parasagittal limb orientation of mammals limits lateral undulations of the body during locomotion (similar to turtles which completely lack lateral undulations), and the loss of the primary articulation between the shoulder and the sternum allows the scapula to act as an additional limb segment that increases stride length (Eaton, 1944). In mammalian species for which three-dimensional movements of the pectoral girdle have been quantified, the pectoral girdle undergoes rotational excursions very similar to those observed in *P. concinna* (cats: ~41°, (Boczek-Funcke, 1996); sloths: ~34°, (Nyakatura and Fischer, 2010)). Two-dimensional studies found similar amounts of rotation in mammals (spider monkey: ~35°, (Jenkins et al., 1978); opossum: ~40°, (Jenkins and Weijs, 1979); dogs: ~35°, goats: ~41°, (Fischer and Blickhan, 2006)), and in humans the contribution of scapular motion to arm elevation has been estimated as approximately 33% of total arm protraction/retraction (Veeger and van der Helm, 2007), similar to turtles. Thus, rather than functioning as a constraint to girdle and limb motion, the loss of lateral undulations of the vertebral column due to the presence of the bony

shell in the turtles may represent a functional convergence with mammals, whereby increased girdle rotations play a greater role in forelimb function than they do in other sprawling taxa.

Acknowledgements: We thank Alysia Arellanez, Catherine Petty, Alison Sansone and Lucy Stevens for their assistance with surgical procedures, David Baier for helpful discussion, and David Baier and Stephen Gatesy for the XROMM MayaTools.

Competing interests: We declare we have no competing interests.

Funding. This research was supported by a Company of Biologists Travel grant to C.J.M; Clemson University Creative Inquiry funds (#479 to R.W.B.); the National Science Foundation (1661129 and 1655756 to E.L.B), and personal funds.

Data accessibility: Data supporting this article can be accessed at https://figshare.com/account/projects/71132/articles/10132916.

Author contributions: Experimental design: C.J.M., J.G.C., R.W.B., J.W. and E.L.B. Performed data collection: All authors. Processed data: C.J.M., J.G.C., A.A.M., E.L.B. Analyzed data: C.J.M. Wrote manuscript: C.J.M. Provided comments on manuscript: J.G.C., A.A.M., R.W.B., J.W. and E.L.B.

References

Alexander, R. M. N. (1974). The mechanics of jumping by a dog (*Canis familiaris*). *J. Zool.* **173**, 549–573.

Ashley-Ross, M. (1994). Hindlimb kinematics during terrestrial locomotion in a salamander (*Dicamptodon tenebrosus*). *J. Exp. Biol.* **193**, 255–83.

Ashley-Ross, M. A. and Bechtel, B. F. (2004). Kinematics of the transition between aquatic and terrestrial locomotion in the newt *Taricha torosa*. *J. Exp. Biol.* **207**, 461–474.

Baier, D. B. and Gatesy, S. M. (2013). Three-dimensional skeletal kinematics of the shoulder girdle and forelimb in walking Alligator. *J. Anat.* **223**, 462–473.

Baier, D. B., Garrity, B. M., Moritz, S. and Carney, R. M. (2018). *Alligator mississippiensis* sternal and shoulder girdle mobility increase stride length during high walks. *J. Exp. Biol.* **221**, jeb186791.

Basu, C., Wilson, A. M. and Hutchinson, J. R. (2019). The locomotor kinematics and ground reaction forces of walking giraffes. *J. Exp. Biol.* **222**, jeb159277.

Bates, D., Mächler, M., Bolker, B. and Walker, S. (2015). Fitting linear mixed-effects models using lme4. *J. Stat. Softw.* **67**, 1–48.

Biewener, A. A. and Patek, S. N. (2018). *Animal Locomotion*. 2nd ed. Oxford, UK: Oxford University Press.

Blob, R. W. and Biewener, A. A. (2001). Mechanics of limb bone loading during terrestrial locomotion in the green iguana (*Iguana iguana*) and American alligator (*Alligator mississippiensis*). *J. Exp. Biol.* **204**, 1099–122.

Blob, R. W., Rivera, A. R. V and Westneat, M. W. (2008). Hindlimb function in turtle locomotion: limb movements and muscular activation across taxa, environment, and ontogeny. In *Biology of turtles* (ed. Wyneken, J.), Godfrey, M.), and Bels, V.), pp. 139–162. Boca Raton, FL: CRC Press.

Boczek-Funcke, A. (1996). Kinematic analysis of the cat shoulder girdle during treadmill locomotion: An X-ray study. *Eur. J. Neurosci.* **8**, 261–272.

Brainerd, E. L., Baier, D. B., Gatesy, S. M., Hedrick, T. L., Metzger, K. A., Gilbert, S. L. and Crisco, J. J. (2010). X-ray reconstruction of moving morphology (XROMM): precision, accuracy and applications in comparative biomechanics research. *J. Exp. Zool. A. Ecol. Genet. Physiol.* **313**, 262–79.

Brainerd, E. L., Blob, R. W., Hedrick, T. L., Creamer, A. T. and Müller, U. K. (2017). Data management rubric for video data in organismal biology. *Integr. Comp. Biol.* **57**, 33–47.

Burke, A. C. (1989). Development of the turtle carapace: implications for the evolution of a novel bauplan. *J. Morphol.* **378**, 363–378.

Butcher, M. T. and Blob, R. W. (2008). Mechanics of limb bone loading during terrestrial locomotion in river cooter turtles (*Pseudemys concinna*). *J. Exp. Biol.* **211**, 1187–1202.

Carrier, D. R. (2006). Locomotor function of the pectoral girdle `muscular sling' in trotting dogs. *J. Exp. Biol.* **209**, 2224–2237.

Chen, J. J., Peattie, A. M., Autumn, K. and Full, R. J. (2006). Differential leg function in a sprawled-posture quadrupedal trotter. *J. Exp. Biol.* **209**, 249–259.

Cieri, R. L., Moritz, S., Capano, J. G. and Brainerd, E. L. (2018). Breathing with floating ribs: XROMM analysis of lung ventilation in savannah monitor lizards. *J. Exp. Biol.* **3**, jeb.189449.

Coates, M. I., Jeffery, J. E. and Ruta, M. (2002). Fins to limbs: What the fossils say. *Evol. Dev.* **4**, 390–401.

Collings, A. J., Porro, L. B., Hill, C. and Richards, C. T. (2019). The impact of pelvic lateral rotation on hindlimb kinematics and stride length in the red-legged running frog, *Kassina maculata*. *R. Soc. Open Sci.* **6**, 190060.

Deban, S. M. and Schilling, N. (2009). Activity of trunk muscles during aquatic and terrestrial locomotion in *Ambystoma maculatum*. *J. Exp. Biol.* **212**, 2949–2959.

Delvolvé, I., Bem, T. and Cabelguen, J. M. (1997). Epaxial and limb muscle activity during swimming and terrestrial stepping in the adult newt, *Pleurodeles waltl*. *J. Neurophysiol.* **78**, 638–650.

Eaton, T. H. (1944). Modifications of the shoulder girdle related to reach and stride in mammals. *J. Morphol.* **75**, 167–171.

Fischer, M. S. and Blickhan, R. (2006). The tri-segmented limbs of Therian mammals: kinematics, dynamics, and self-stabilization— a review. *J. Exp. Zool.* **305A**, 935–952.

Fischer, M. S., Krause, C. and Lilje, K. E. (2010). Evolution of chameleon locomotion, or how to become arboreal as a reptile. *Zoology* **113**, 67–74.

Fish, F. E. (1984). Kinematics of undulatory swimming in the American alligator. *Copeia* **1984**, 839–843.

Gillis, G. B. and Blob, R. W. (2001). How muscles accommodate movement in different physical environments: aquatic vs. terrestrial locomotion in vertebrates. *Comp. Biochem. Physiol. Part A* **131**, 61–75.

Griffin, T. M., Main, R. P. and Farley, C. T. (2004). Biomechanics of quadrupedal walking: how do four-legged animals achieve inverted pendulum-like movements? *J. Exp. Biol.* **207**, 3545–3558.

Jastrebsky, R. A., Bartol, I. K. and Krueger, P. S. (2016). Turning performance in squid and cuttlefish: unique dual-mode muscular hydrostatic systems. *J. Exp. Biol.* **219**, 1317–1326.

Jenkins, F. A. and Goslow Jr., G. E. (1983). The functional anatomy of the shoulder of the savannah monitor lizard (*Varanus exanthematicus*). *J. Morphol.* **175**, 195–216.

Jenkins, F. A. and Weijs, W. A. (1979). The functional anatomy of the shoulder in the Virginia opossum (*Didelphis virginiana*). *J. Zool. Soc. London* **188**, 379–410.

Jenkins, F. A., Dombrowski, P. J. and Gordon, E. P. (1978). Analysis of the shoulder in brachiating spider monkeys. *Am. J. Phys. Anthropol.* **48**, 65–76.

Kambic, R. E., Roberts, T. J. and Gatesy, S. M. (2014). Long-axis rotation: a missing degree of freedom in avian bipedal locomotion. *J. Exp. Biol.* **217**, 2770–2782.

Kambic, R. E., Roberts, T. J. and Gatesy, S. M. (2015). Guineafowl with a twist: asymmetric limb control in steady bipedal locomotion. *J. Exp. Biol.* **218**, 3836–3844.

Knörlein, B. J., Baier, D. B., Gatesy, S. M., Laurence-Chasen, J. D. and Brainerd, E. L. (2016). Validation of XMALab software for marker-based XROMM. *J. Exp. Biol.* **219**, 3701–3711.

Lindgren, J., Caldwell, M. W., Konishi, T. and Chiappe, L. M. (2010). Convergent evolution in aquatic tetrapods: Insights from an exceptional fossil mosasaur. *PLoS One* **5**, 1–10.

Mayerl, C. J., Brainerd, E. L. and Blob, R. W. (2016). Pelvic girdle mobility of cryptodire and pleurodire turtles during walking and swimming. *J. Exp. Biol.* **219**, 2650–2658.

Mayerl, C. J., Pruett, J. E., Summerlin, M. N., Rivera, A. R. V and Blob, R. W. (2017). Hindlimb muscle function in turtles: is novel skeletal design correlated with novel muscle function? *J. Exp. Biol.* **220**, 2554–2562.

Mayerl, C. J., Youngblood, J. P., Rivera, G., Vance, J. T. and Blob, R. W. (2019). Variation in morphology and kinematics underlies variation in swimming stability and turning performance in freshwater turtles. *Integr. Org. Biol.* **1**,.

McElroy, E. J., Wilson, R., Biknevicius, A. R. and Reilly, S. M. (2014). A comparative study of single-leg ground reaction forces in running lizards. *J. Exp. Biol.* **217**, 735–742.

Menegaz, R. A., Baier, D. B., Metzger, K. A., Herring, S. W. and Brainerd, E. L. (2015). XROMM analysis of tooth occlusion and temporomandibular joint kinematics during feeding in juvenile miniature pigs. *J. Exp. Biol.* **218**, 2573–2584.

Nagashima, H., Sugahara, F., Takechi, M., Ericsson, R., Kawashima-Ohya, Y., Narita, Y. and Kuratani, S. (2009). Evolution of the Turtle body plan by the folding and creation of new muscle connections. *Science (80-.).* **325**, 193–197.

Nyakatura, J. A. and Fischer, M. S. (2010). Three-dimensional kinematic analysis of the pectoral girdle during upside-down locomotion of two-toed sloths (*Choloepus didactylus*, Linné 1758). *Front. Zool.* **7**, 1–16.

Pace, C. M., Blob, R. W. and Westneat, M. W. (2001). Comparative kinematics of the forelimb during swimming in red-eared slider (*Trachemys scripta*) and spiny softshell (*Apalone spinifera*) turtles. *J. Exp. Biol.* **204**, 3261–3271.

Peters, S. and Goslow Jr., G. E. (1983). From salamanders to mammals: continuity in musculoskeletal function during locomotion. *Brain. Behav. Evol.* **22**, 191–197.

Pridmore, P. A. (1992). Trunk movements during locomotion in the marsupial *Monodelphis domestica* (Didelphidae). *J. Morphol.* **211**, 137–146.

Raichlen, D. A., Pontzer, H., Shapiro, L. J. and Sockol, M. D. (2009). Understanding hind limb weight support in chimpanzees with implications for the evolution of primate locomotion. *Am. J. Phys. Anthropol.* **138**, 395–402.

Reilly, S. and Delancey, M. (1997). Sprawling locomotion in the lizard *Sceloporus clarkii*: the effects of speed on gait, hindlimb kinematics, and axial bending during walking. *J. Zool.* **243**, 417–433.

Rewcastle, S. C. (1983). Fundamental adaptations in the lacertilian hind limb : a partial analysis of the sprawling limb posture and gait. *Copeia* **1983**, 476–487.

Ringma, J. L. and Salisbury, S. W. (2014). Aquatic locomotor kinematics of the eastern water dragon (*Intellagama lesueurii*). *J. Herpetol.* **48**, 240–248.

Rivera, A. R. V and Blob, R. W. (2010). Forelimb kinematics and motor patterns of the slider turtle

(*Trachemys scripta*) during swimming and walking: shared and novel strategies for meeting locomotor demands of water and land. *J. Exp. Biol.* **213**, 3515–26.

Rivera, G., Rivera, A. R. V, Dougherty, E. E. and Blob, R. W. (2006). Aquatic turning performance of painted turtles (*Chrysemys picta*) and functional consequences of a rigid body design. *J. Exp. Biol.* **209**, 4203–13.

Schmidt, M., Mehlhorn, M. and Fischer, M. S. (2016). Shoulder girdle rotation , forelimb movement , and the influence of carapace shape on locomotion in *Testudo hermanni* (Testudinidae). *J. Exp. Biol.* 2693–2703.

Sefati, S., Neveln, I. D., Roth, E., Mitchell, T. R. T., Snyder, J. B., Maciver, M. A., Fortune, E. S. and Cowan, N. J. (2013). Mutually opposing forces during locomotion can eliminate the tradeoff between maneuverability and stability. *Proc. Natl. Acad. Sci.* **110**, 18798–18803.

Shine, C. L., Penberthy, S., Robbins, C. T., Nelson, O. L. and McGowan, C. P. (2015). Grizzly bear (*Ursus arctos horribilis*) locomotion: gaits and ground reaction forces. *J. Exp. Biol.* **218**, 3102–3109.

Veeger, H. E. J. and van der Helm, F. C. T. (2007). Shoulder function: The perfect compromise between mobility and stability. *J. Biomech.* **40**, 2119–2129.

Walker, W. F. (1971). A structural and functional analysis of walking in the turtle, *Chrysemys picta marginata*. *J. Morphol.* **134**, 195–213.

Walker, W. F. (1973). The locomotor apparatus of testudines. In *Biology of the Reptilia. Vol. IV. Morphology, part D* (ed. Gans, C.) and Parsons, T.), pp. 1–100. New York: Academic Press.

Willey, J. S., Biknevicius, A. R., Reilly, S. M. and Earls, K. D. (2004). The tale of the tail: limb function and locomotor mechanics in *Alligator mississippiensis*. *J. Exp. Biol.* **207**, 553–563.

Xu, R. (2003). Measuring explained variation in linear mixed effects models. *Stat. Med.* **22**, 3527–3541.

Young, V. K. H. and Blob, R. W. (2015). Limb bone loading in swimming turtles: changes in loading facilitate transitions from tubular to flipper-shaped limbs during aquatic invasions. *Biol. Lett.* **11**, 1–5.

Young, V. K. H., Wienands, C. E., Wilburn, B. P. and Blob, R. W. (2017). Humeral loads during swimming and walking in turtles: implications for morphological change during aquatic reinvasions. *J. Exp. Biol.* jeb.156836.

Zani, P. A., Gottschall, J. S. and Kram, R. (2005). Giant Galapagos tortoises walk without inverted pendulum mechanical-energy exchange. *J. Exp. Biol.* **208**, 1489–94.

Zug, G. R. (1972). Walk pattern analysis of cryptodiran turtle gaits. *Anim. Behav.* **20**, 439–443.

Figures and Tables

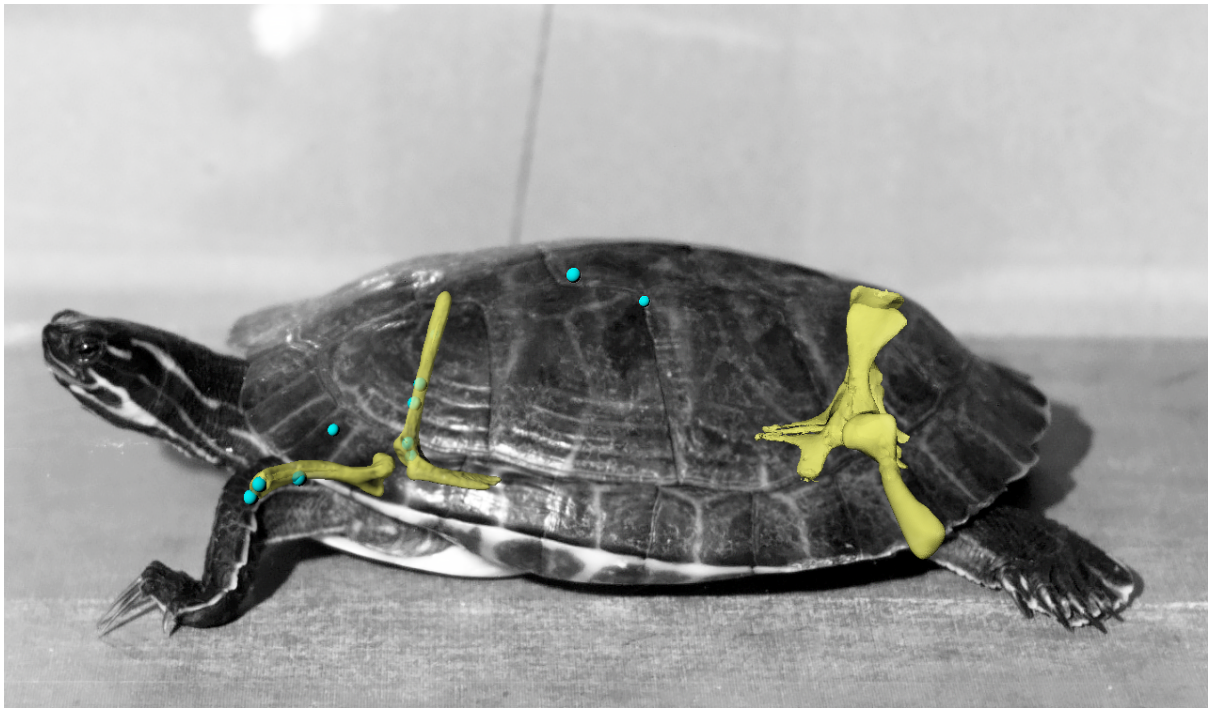

Figure 1. The fore- and hind limb apparatus of *Pseudemys concinna*, with marker placements for the forelimb and shell in blue. The left and right sides of the pelvic girdle are ankylosed together and function as a single structure, whereas the pectoral girdle of each side functions independently from the other. Hindlimb marker locations are detailed in Mayerl et al., (2016).

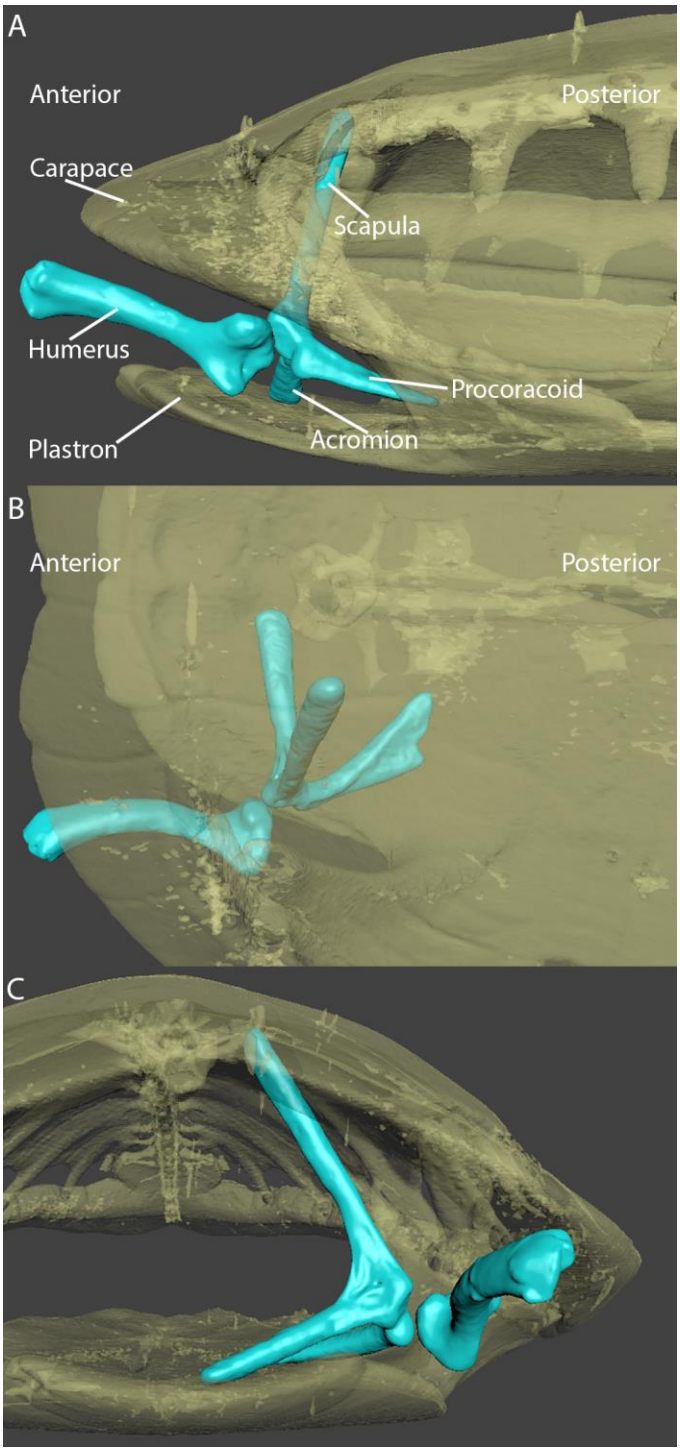

Figure 2. Forelimb orientation of *P. concinna* in lateral (A), dorsoventral (B) and anterior (C) views when the humerus is protracted to be parallel to the long axis of the shell. The girdle lies deep to the shell. The procoracoid process is contained within the Pectoralis-Supracoracoideus-Coracobrachialis magnus muscle mass. In addition to several the muscular connections between the shell and girdle,

the acromion process has a ligamentous connection to the plastron, and the scapula attaches to the medial pleural bones and anterior trunk vertebrae via suprascapular cartilages. During locomotion, the girdle rotates primarily through yaw.

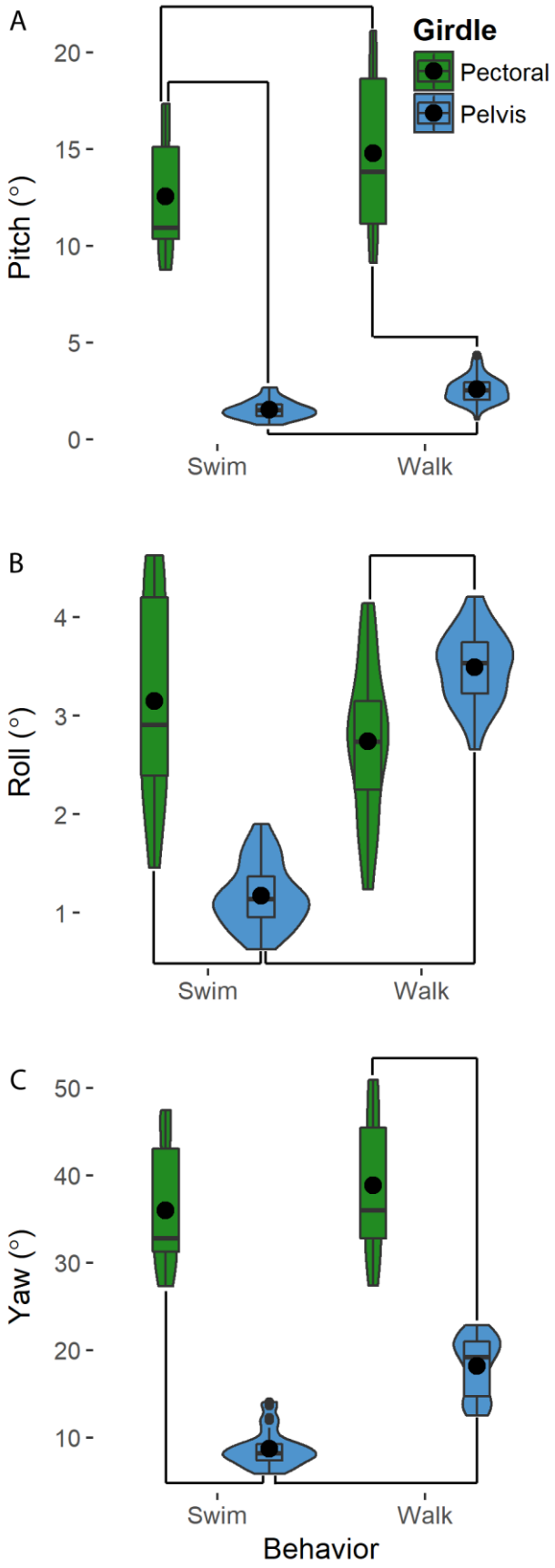

Figure 3. Mean pectoral (green) and pelvic (blue) girdle rotational excursions throughout a limb cycle during swimming and walking for pitch (A), roll (B) and yaw (C) motions relative to the shell. Lines indicate significant differences between swimming and walking within each girdle or between girdles within a behavior. Large black dots: mean values; small black dots: outliers; width of plot on x-axis: frequency distribution of data along the y-axis; box and whisker plots indicate the median interquartile range (IQR), with whiskers indicating 1.5 * IQR in either direction.

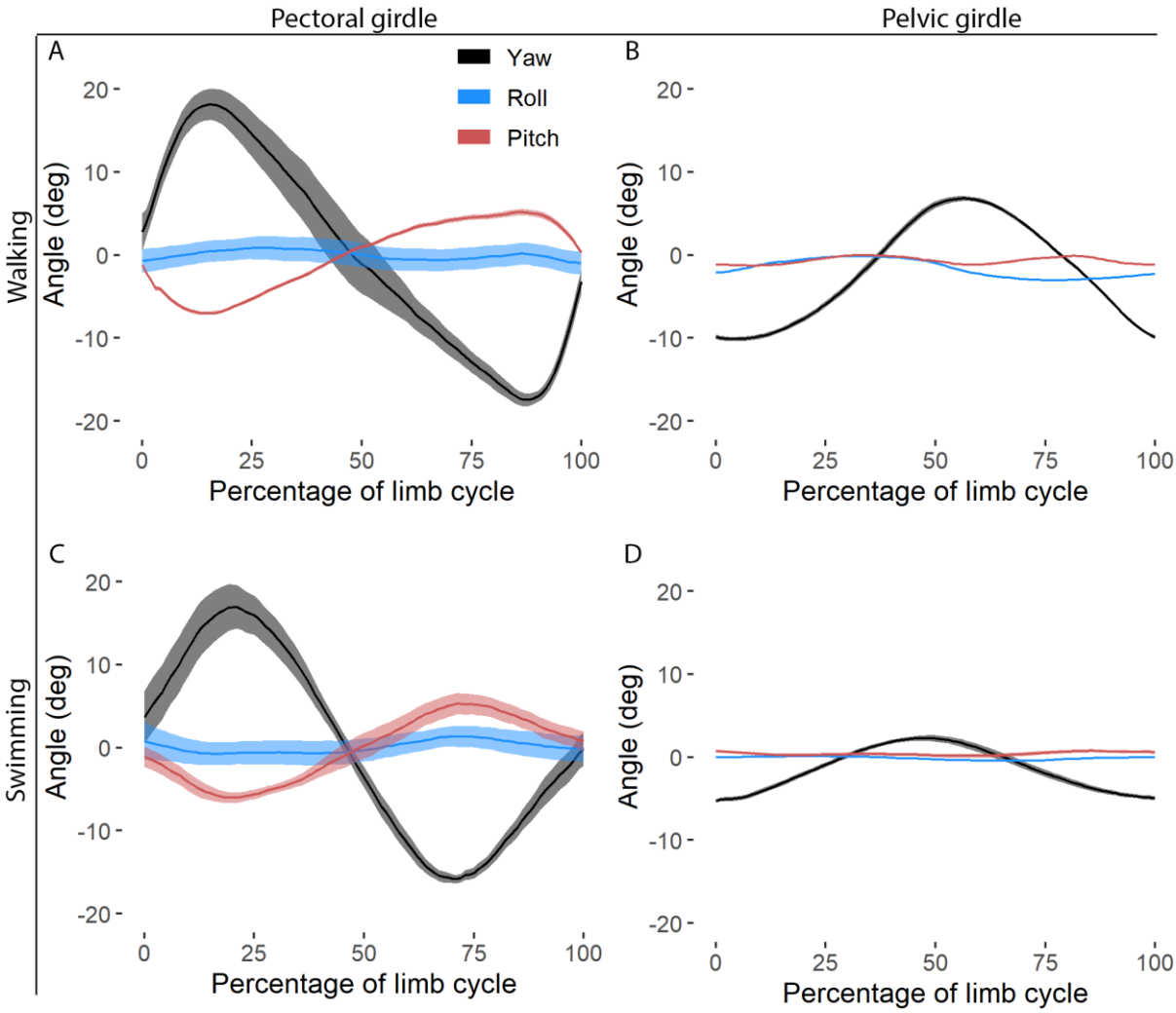

Figure 4. Mean girdle rotations (solid line) ± SE (transparent areas) through a limb cycle in yaw (black), roll (blue) and pitch (red) of the pectoral girdle (A,C) and pelvic girdle (B,D) during walking (top, A,B) and swimming (bottom, C,D).

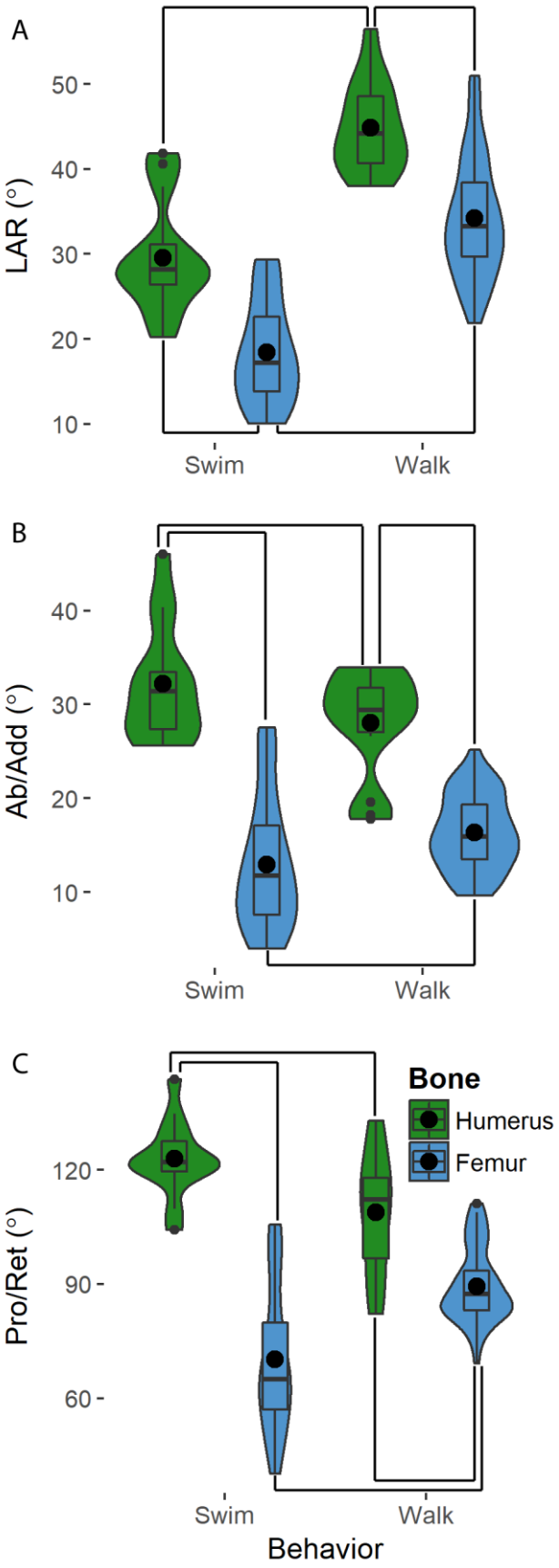

Figure 5. Mean humeral (green) and femoral (blue) excursions throughout a limb cycle relative to the girdle-limb joint during swimming and walking for long axis rotation (A, LAR), abduction/adduction (B, Ab/Add), and protraction/retraction (C, Pro/Ret) motions. Lines indicate significant differences between swimming and walking within each girdle or between girdles within a behavior. Large black dots: mean values; small black dots: outliers; width of plot on x-axis: frequency distribution of data along the y-axis; box and whisker plots indicate the median interquartile range (IQR), with whiskers indicating 1.5 * IQR in either direction.

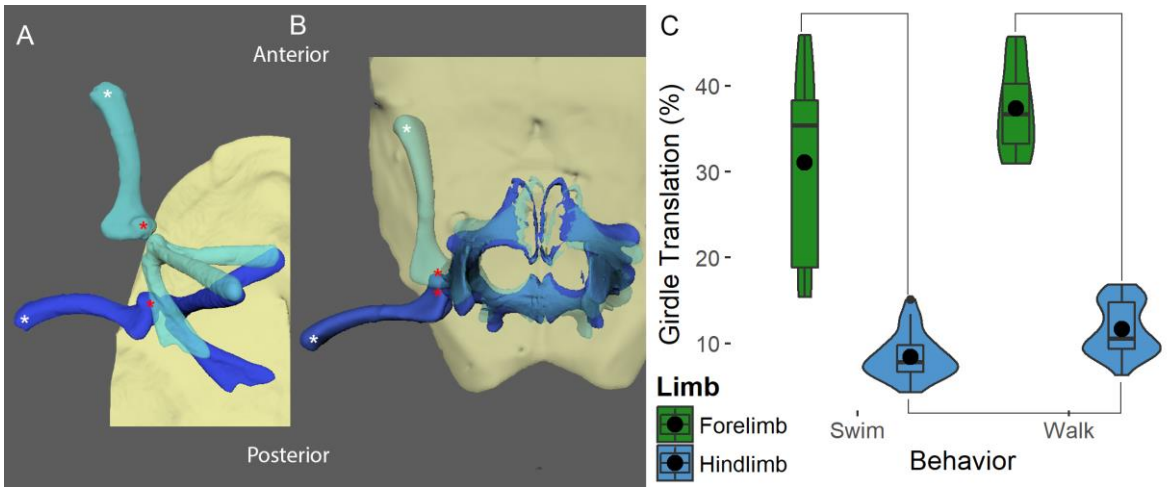

Figure 6. The contributions of girdle rotations to humeral (A, C [green]) and femoral (B, C [blue]) protraction/retraction. A and B present example steps in the forelimb (A) and hind limb (B), with the most protracted position of the limb indicated by the teal, and the most retracted position of the limb indicated by the dark blue. Red asterisk: center of the humeral head (A) and femoral head (B) at both points; white asterisk: center of the distal tip of the humerus (A) and femur (B) at both time points; in (C), lines indicate statistically significant differences between groups; large black dots: mean values; small black dots: outliers; width of plot on x-axis: frequency distribution of data along the y-axis; box and whisker plots indicate the median interquartile range (IQR), with whiskers indicating 1.5 * IQR in either direction.

Table 1. Mean ± SE Rotational excursion of the shoulder and pelvic girdles during swimming and walking.

	Shoulder		Pelvis		Ω^2	P value		
	Swim (N = 13)	Walk (N = 15)	Swim (N = 30)	Walk (N = 54)		Limb	Behavior	Limb * Behavior
Rx, 'pitch'	12.6 ± 0.7	14.8 ± 0.7	1.5 ± 0.6	2.6 ± 0.5	**0.90**	**<0.001**	**<0.001**	0.14
Ry, 'roll'	3.15 ± 0.2	2.74 ± 0.1	1.2 ± 0.1	3.5 ± 0.1	**0.77**	NA	NA	**<0.001**
Rz, 'yaw'	36.2 ± 2.2	38.9 ± 2.2	8.6 ± 2.0	18.2 ± 1.9	**0.90**	NA	NA	**<0.001**

Ω^2: Measure of effects size of the model (Variable ~ Girdle + Behavior + Girdle*Behavior + (1|Turtle)).

Bolded values indicate statistically significant values.

Table 2. Mean ± SE pectoral and pelvic girdle contributions to overall limb excursion.

	Pectoral		Pelvic		Ω^2	P value		
	Swim (N = 13)	Walk (N = 14)	Swim (N = 30)	Walk (N = 49)		Limb	Behavior	Limb * behavior
Girdle Contribution	31.2 ± 1.7%	37.5 ± 1.7%	8.2 ± 1.4	11.6 ± 1.3	**0.85**	**<0.001**	**<0.001**	0.15

Ω^2: Measure of effects size of the model (Girdle Contribution ~ Limb + Behavior + Limb*Behavior + (1|Turtle)).

Bolded values indicate statistically significant differences between groups.

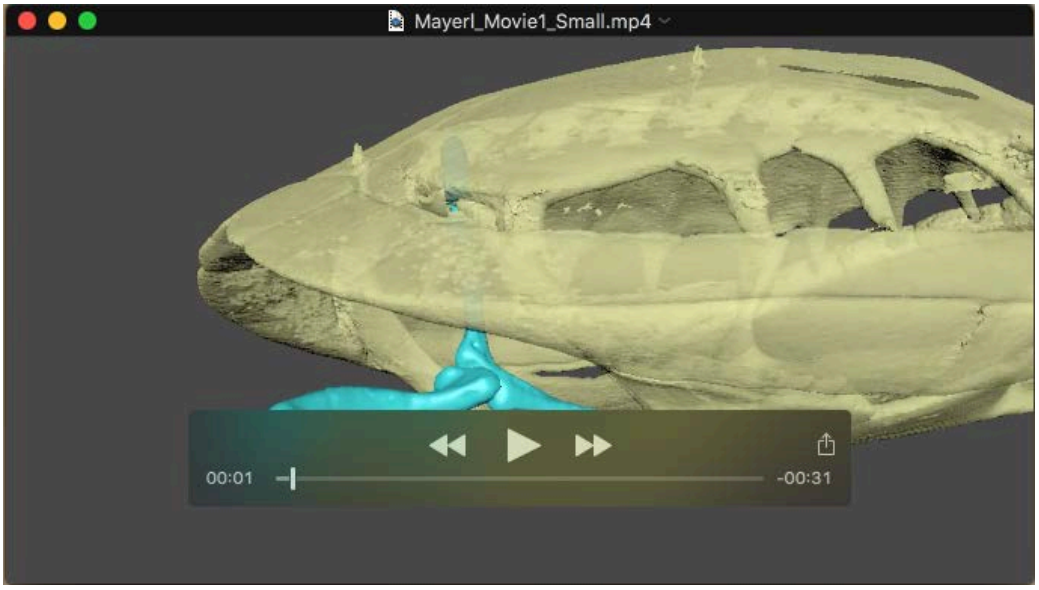

Movie 1. XROMM animation of the pectoral girdle and humerus of *Pseudemys concinna* walking from a lateral view (first three steps) and a dorsal view (last three steps).

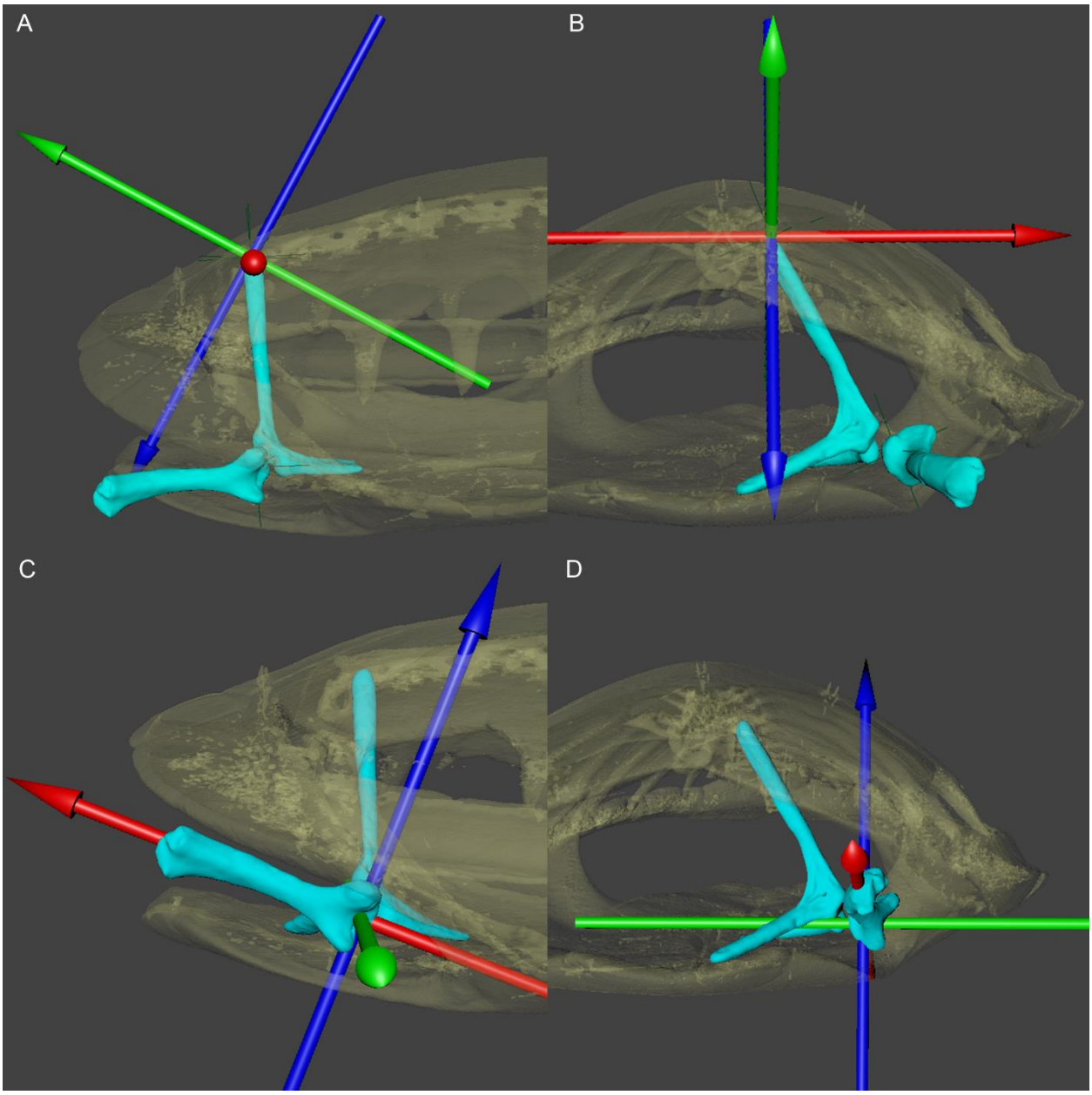

Figure S1. Joint coordinate system for the pectoral girdle (A,B) and humerus (C,D) in *Pseudemys concinna* in lateral (left) and anterior (right) views. Axis orientations for the pectoral girdle were set so that rotation about the x axis (red) measures pitch, rotation about the y-axis (green) measures roll, and rotation about the z-axis (blue) measures yaw. Movements of the pectoral girdle were measured relative to the shell. Axis orientations for the humerus were set so that rotation about the x axis (red) measures long-axis rotation, rotation about the y-axis (green) measures abduction/adduction, and rotation about the z-axis (blue) measures protraction/retraction. Movements of the humerus were measured relative to the pectoral girdle.

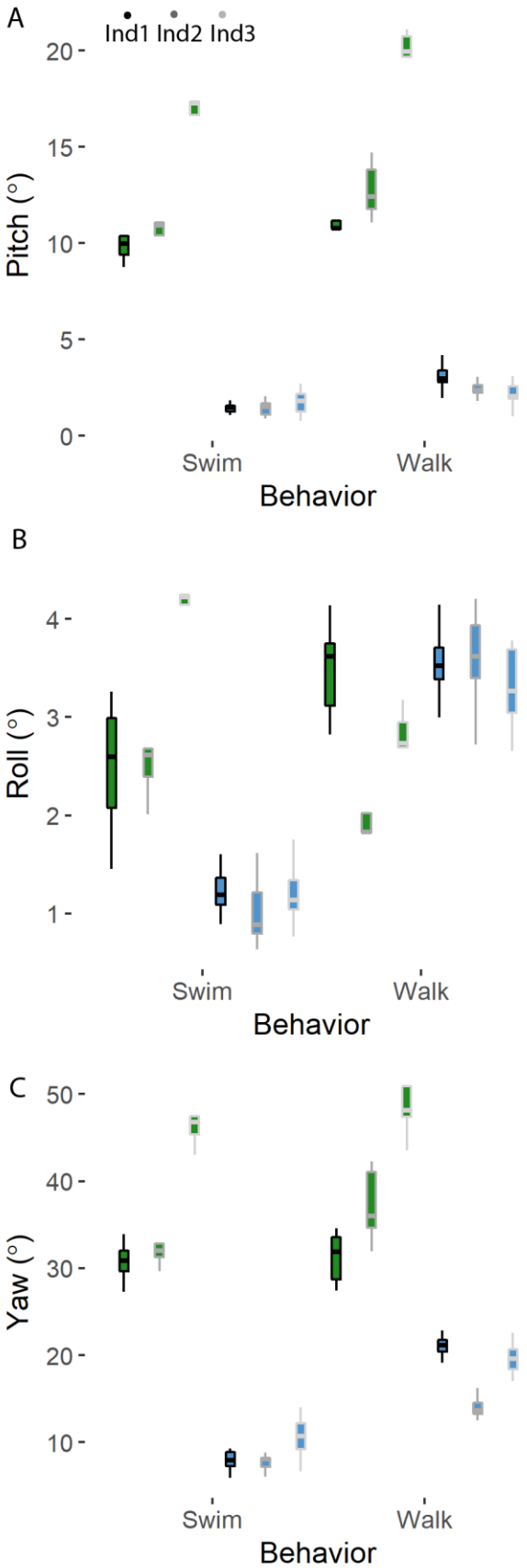

Figure S2. Girdle rotations for individual turtles during walking and swimming for pitch (A), roll (B) and yaw (C) movements. Green box and whisker plots indicate shoulder movements; blue box and whisker plots indicate pelvic girdle movements.

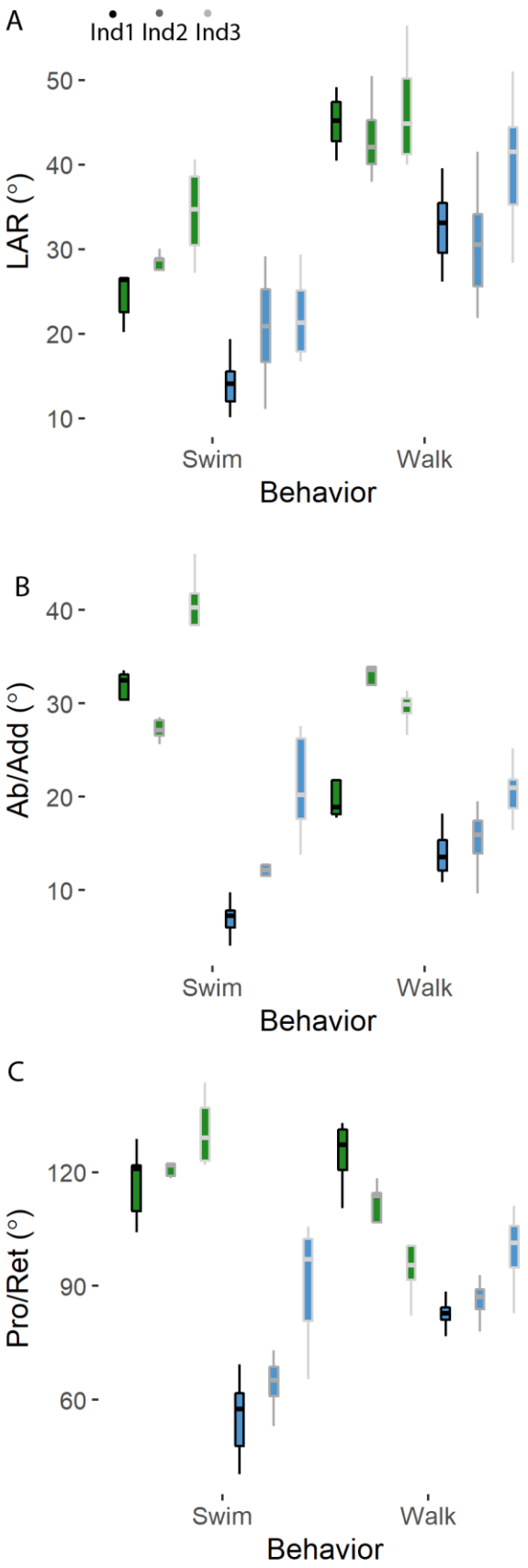

Figure S3. Limb rotations for individual turtles during walking and swimming for LAR (A) Abduction/ Adduction (B) and Protraction/Retraction (C). Green box and whisker plots indicate humeral movements; blue box and whisker plots indicate femoral movements.

Table S1. Tukey's post-hoc analyses for girdle movements in which the behavior * girdle interaction was significant (N = 107).

	Ry, 'roll' (value, p)	Rz, 'Yaw'
SS - PS	**1.98, <0.001**	**27.64, <0.001**
SW – PW	-0.34, 0.17	**18.02, <0.001**
SS – SW	0.41, 0.19	-2.64, 0.23
PS - PW	**-2.32, <0.001**	**-9.62, <0.001**

SS: Shoulder movements during swimming; PS: pelvis movements during swims; SW: shoulder movements during walking; PW: pelvis movements during walking

Bolded values indicate statistically significant differences between groups.

Table S2. Mean +/- SE Rotational excursion of the humerus and femur during swimming and walking.

	Humerus		Femur		Ω^2	p-value		
	Swim (N = 14)	Walk (N = 14)	Swim (N = 30)	Walk (N = 50)		Limb	Behavior	Limb * behavior
Rx, 'LAR'	29.9 ± 2.7	44.7 ± 2.7	18.4 ± 2.4	34.3 ± 2.4	**0.74**	**<0.001**	**<0.001**	0.67
Ry, 'Ab/add'	32.6 ± 2.9	27.8 ± 2.9	13.2 ± 2.8	16.5 ± 2.8	**0.82**	NA	NA	**<0.001**
Rz, 'Pro/ret'	123.6 ± 2.9	108.3 ± 5.9	70.4 ± 5.5	89.6 ± 5.3	**0.73**	NA	NA	**<0.001**

Ω^2: Measure of effects size of the model (Variable ~ Limb + Behavior + Limb*Behavior + (1|Turtle))

Bolded values indicate statistically significant differences between groups.

Table S3. Tukey's post hoc results on limb rotations for limb movements in which the behavior * limb interaction was significant (N = 103).

	Ry, Add/ab	Rz, Pro/ret
HS-FS	**19.41, <0.001**	**53.21, <0.001**
HW-FW	**11.30, <0.001**	**18.70, <0.001**
HS-HW	**4.82, 0.006**	**15.32, 0.004**
FS-FW	**-3.30, 0.001**	**-19.20, <0.001**

HS: Humeral rotations during swimming; HW: humeral rotations during walking; FS: femoral movements during swimming; FW: femoral movements during walking

Bolded values indicate statistically significant differences between groups.

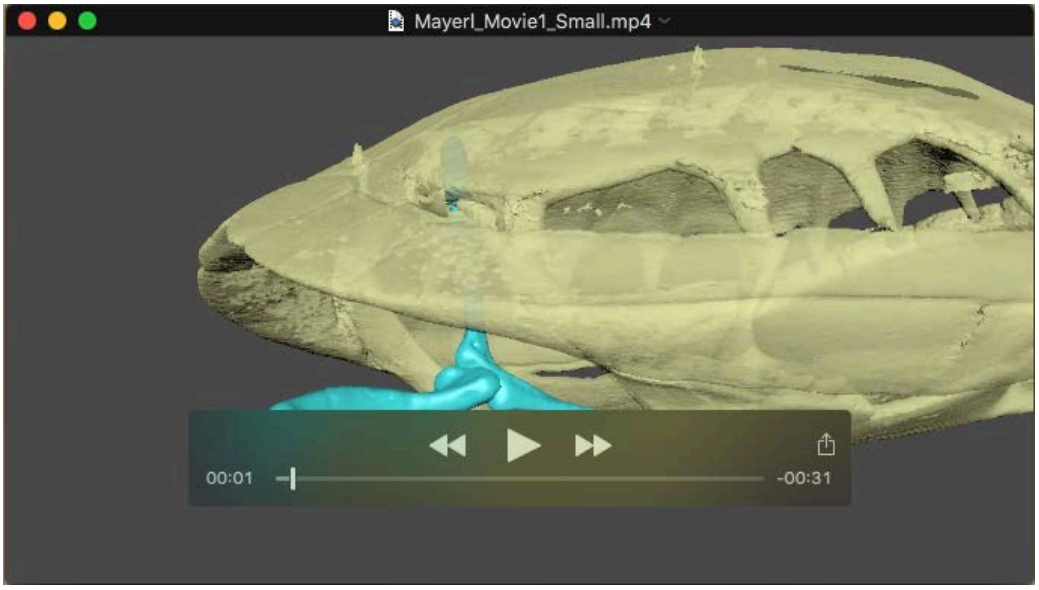

Movie 1. XROMM animation of the pectoral girdle and humerus of *Pseudemys concinna* walking from a lateral view (first three steps) and a dorsal view (last three steps).

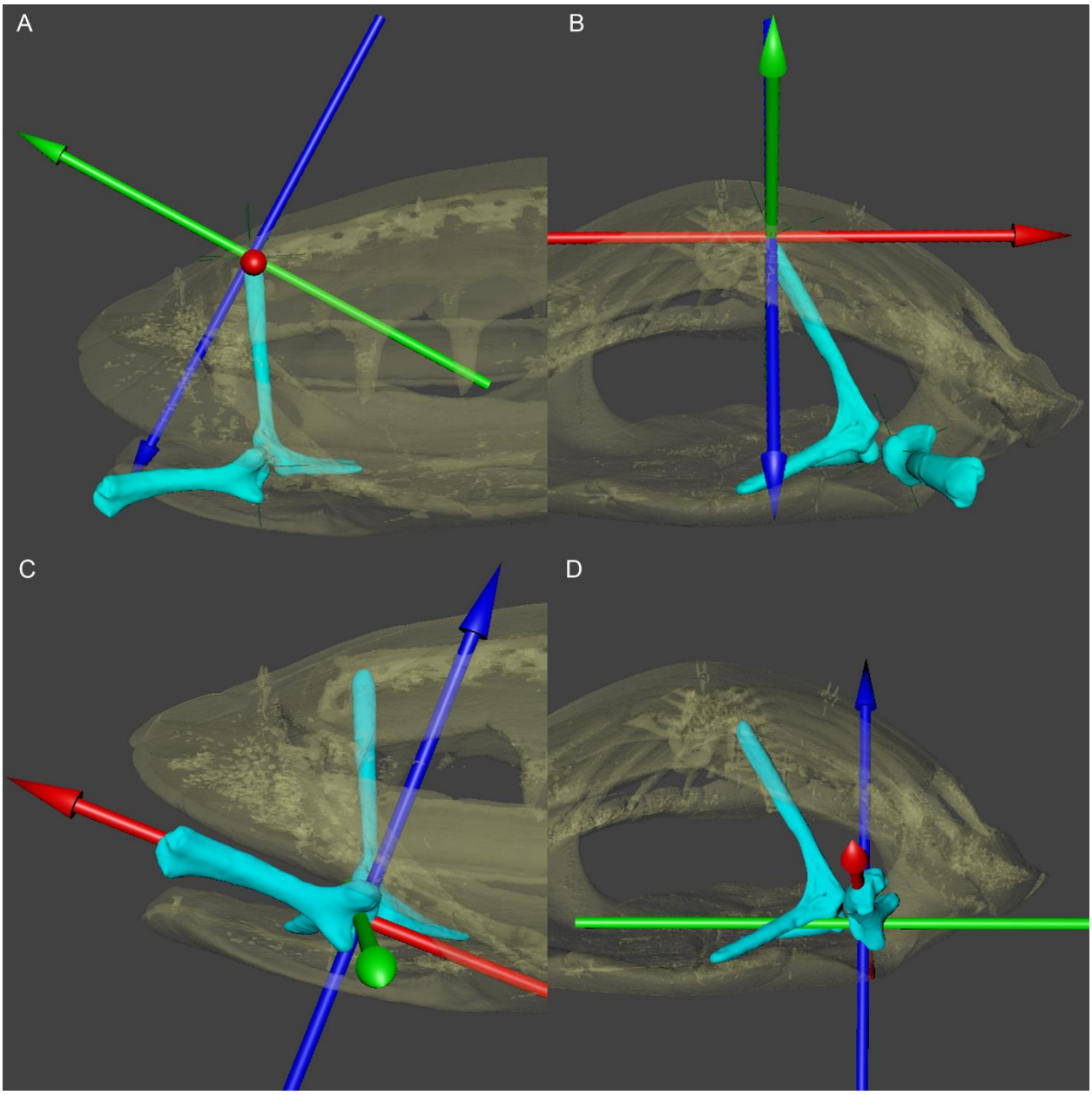

Figure S1. Joint coordinate system for the pectoral girdle (A,B) and humerus (C,D) in *Pseudemys concinna* in lateral (left) and anterior (right) views. Axis orientations for the pectoral girdle were set so that rotation about the x axis (red) measures pitch, rotation about the y-axis (green) measures roll, and rotation about the z-axis (blue) measures yaw. Movements of the pectoral girdle were measured relative to the shell. Axis orientations for the humerus were set so that rotation about the x axis (red) measures long-axis rotation, rotation about the y-axis (green) measures abduction/adduction, and rotation about the z-axis (blue) measures protraction/retraction. Movements of the humerus were measured relative to the pectoral girdle.

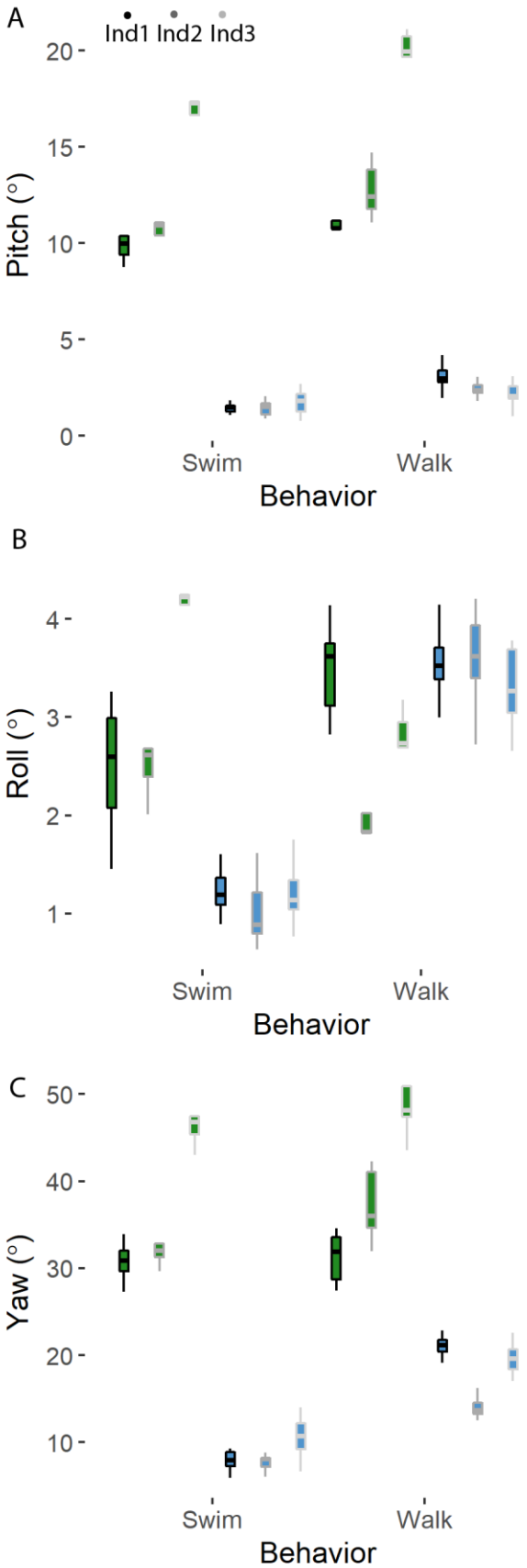

Figure S2. Girdle rotations for individual turtles during walking and swimming for pitch (A), roll (B) and yaw (C) movements. Green box and whisker plots indicate shoulder movements; blue box and whisker plots indicate pelvic girdle movements.

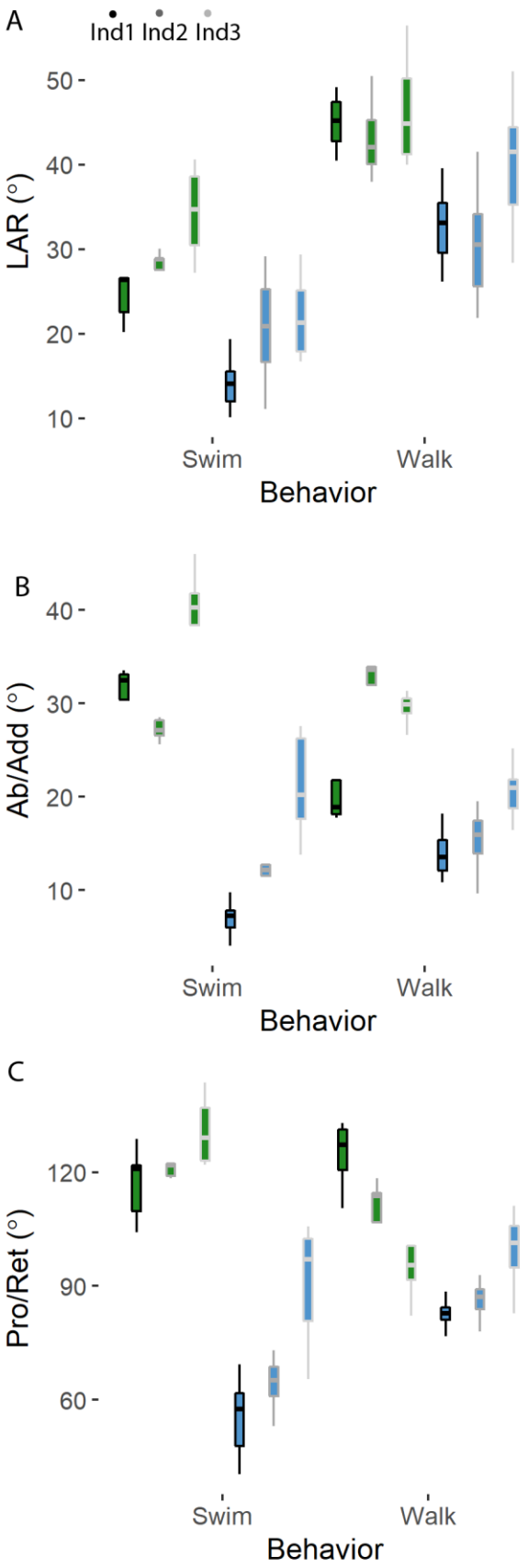

Figure S3. Limb rotations for individual turtles during walking and swimming for LAR (A) Abduction/ Adduction (B) and Protraction/Retraction (C). Green box and whisker plots indicate humeral movements; blue box and whisker plots indicate femoral movements.

Table S1. Tukey's post-hoc analyses for girdle movements in which the behavior * girdle interaction was significant (N = 107).

	Ry, 'roll' (value, p)	Rz, 'Yaw'
SS - PS	**1.98, <0.001**	**27.64, <0.001**
SW – PW	-0.34, 0.17	**18.02, <0.001**
SS – SW	0.41, 0.19	-2.64, 0.23
PS - PW	**-2.32, <0.001**	**-9.62, <0.001**

SS: Shoulder movements during swimming; PS: pelvis movements during swims; SW: shoulder movements during walking; PW: pelvis movements during walking

Bolded values indicate statistically significant differences between groups.

Table S2. Mean +/- SE Rotational excursion of the humerus and femur during swimming and walking.

	Humerus		Femur		Ω^2	p-value		
	Swim (N = 14)	Walk (N = 14)	Swim (N = 30)	Walk (N = 50)		Limb	Behavior	Limb * behavior
Rx, 'LAR'	29.9 ± 2.7	44.7 ± 2.7	18.4 ± 2.4	34.3 ± 2.4	**0.74**	**<0.001**	**<0.001**	0.67
Ry, 'Ab/add'	32.6 ± 2.9	27.8 ± 2.9	13.2 ± 2.8	16.5 ± 2.8	**0.82**	NA	NA	**<0.001**
Rz, 'Pro/ret'	123.6 ± 2.9	108.3 ± 5.9	70.4 ± 5.5	89.6 ± 5.3	**0.73**	NA	NA	**<0.001**

Ω^2: Measure of effects size of the model (Variable ~ Limb + Behavior + Limb*Behavior + (1|Turtle))

Bolded values indicate statistically significant differences between groups.

Table S3. Tukey's post hoc results on limb rotations for limb movements in which the behavior * limb interaction was significant (N = 103).

	Ry, Add/ab	Rz, Pro/ret
HS-FS	**19.41, <0.001**	**53.21, <0.001**
HW-FW	**11.30, <0.001**	**18.70, <0.001**
HS-HW	**4.82, 0.006**	**15.32, 0.004**
FS-FW	**-3.30, 0.001**	**-19.20, <0.001**

HS: Humeral rotations during swimming; HW: humeral rotations during walking; FS: femoral movements during swimming; FW: femoral movements during walking

Bolded values indicate statistically significant differences between groups.